



PROJECT MUSE®

Experimental Flights Using a Small Unmanned Aircraft System for Mapping Emergent Sandbars

Paul Kinzel, Mark Bauer, Mark Feller, Christopher Holmquist-Johnson, Todd Preston



Great Plains Research, Volume 25, Number 1, Spring 2015, pp. 39-52
(Article)

Published by University of Nebraska Press
DOI: 10.1353/gpr.2015.0018

➔ For additional information about this article

<http://muse.jhu.edu/journals/gpr/summary/v025/25.1.kinzel.html>

Experimental Flights Using a Small Unmanned Aircraft System for Mapping Emergent Sandbars

Paul Kinzel, Mark Bauer, Mark Feller,
Christopher Holmquist-Johnson, and Todd Preston

ABSTRACT—The US Geological Survey and Parallel Inc. conducted experimental flights with the Tarantula Hawk (T-Hawk) unmanned aircraft system (UAS) at the Dyer and Cottonwood Ranch properties located along reaches of the Platte River near Overton, Nebraska, in July 2013. We equipped the T-Hawk UAS platform with a consumer-grade digital camera to collect imagery of emergent sandbars in the reaches and used photogrammetric software and surveyed control points to generate orthophotographs and digital elevation models (DEMs) of the reaches. To optimize the image alignment process, we retained and/or eliminated tie points based on their relative errors and spatial resolution, whereby minimizing the total error in the project. Additionally, we collected seven transects that traversed emergent sandbars concurrently with global positioning system location data to evaluate the accuracy of the UAS survey methodology. The root mean square errors for the elevation of emergent points along each transect across the DEMs ranged from 0.04 to 0.12 m. If adequate survey control is established, a UAS combined with photogrammetry software shows promise for accurate monitoring of emergent sandbar morphology and river management activities in short (1–2 km) river reaches.

Key Words: fluvial geomorphology, remote sensing, riverine habitat, sandbars, unmanned aircraft systems

Introduction

The use of unmanned aircraft systems (UAS) in the United States is anticipated to increase once the Federal Aviation Administration (FAA) develops guidelines to permit their widespread integration into the National Airspace System (NAS). Once these regulations are established, it is anticipated that UAS technology will be used for a variety of civilian applications including environmental monitoring (Ball 2013). Currently, universities, commercial companies, and government operators of unmanned aircraft systems in the NAS can apply for a certificate of authorization from the FAA. The authorization process also requires a radio spectrum approval from the National Telecommunications and Information Administration. The United States Geological Survey (USGS) National UAS Project Office routinely obtains

authorization for utilizing UAS technology for a variety of environmental monitoring applications for the US Department of the Interior (<http://rmgsc.cr.usgs.gov/uas/>). Technical developments in UAS hardware, sensors, post-processing software, and workflow are rapidly advancing and have the potential to provide scientists with cost-effective mapping and imaging tools for environmental monitoring, including river applications (Lejot et al. 2007).

A river application relevant for natural resource managers in the Great Plains is monitoring emergent sandbar nesting habitat for endangered and threatened species including the interior least tern (*Sterna antillarum athalassos*) and piping plover (*Charadrius melodus*). Various remote sensing platforms and imagers have been used to delineate the areal extent of sandbar features. These include conventional aerial photography (Elliott et al. 2009; Elliott 2011), multispectral satellite imagery (Strong 2007), hyperspectral imaging (Legleiter et al. 2011), and midwave thermal-infrared imaging (Kinzel et al. 2009). However, single images provide

.....
Manuscript received for review, 1/14/14;

accepted for publication, 7/3/14.

Great Plains Research 25 (Spring 2015):39–52. Copyright © 2015 by the
Center for Great Plains Studies, University of Nebraska–Lincoln
.....

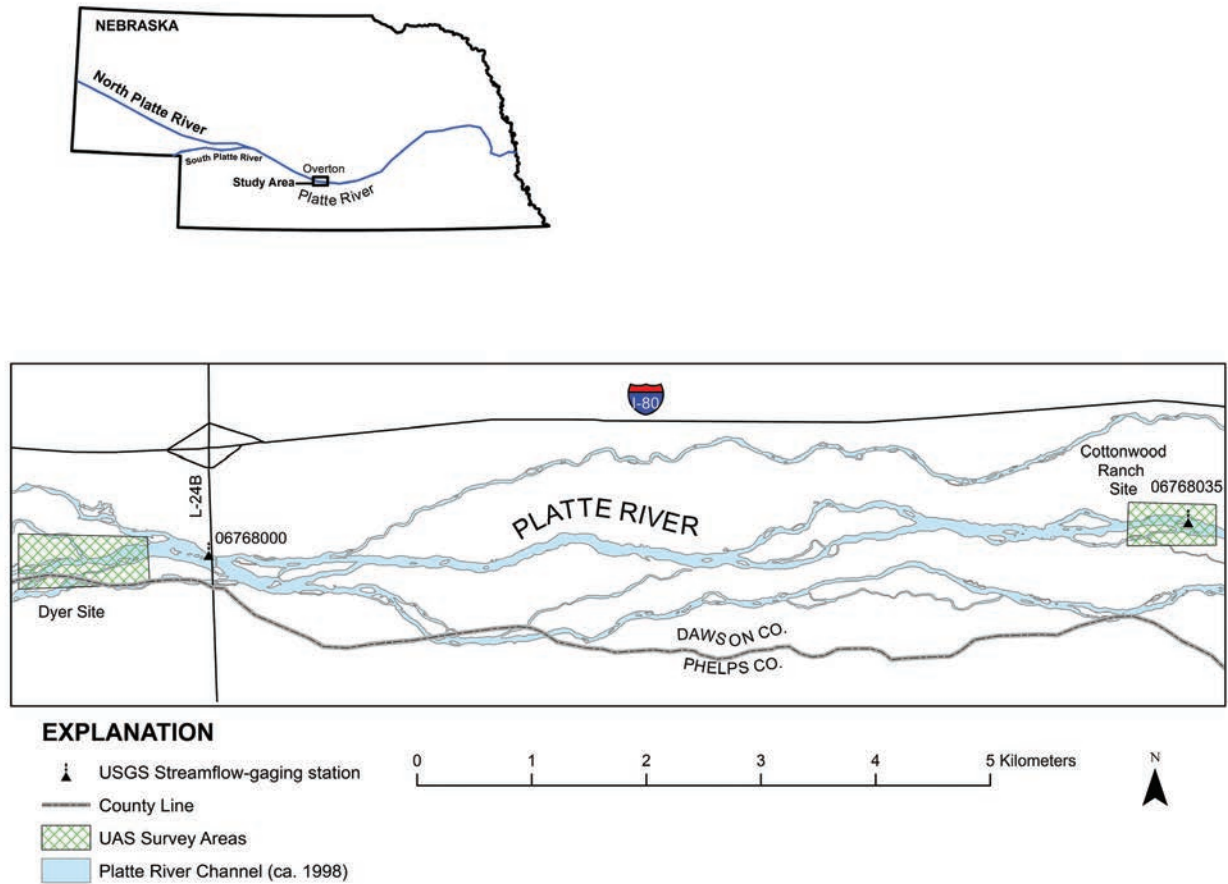


Figure 1. Map showing the location of the unmanned aircraft system (UAS) survey areas.

limited information on the vertical structure of these habitats, information which is critical to understanding the potential risk, frequency, or spatial extent of inundation. Further, sandbars are dynamic fluvial landforms sculpted by the ebb and flow of water and influenced by floods and upstream sediment supply. For this reason, monitoring their spatial and temporal evolution in response to natural events and/or management activities is a challenging endeavor.

High-resolution topographic mapping with aerial Light Detection and Ranging (LiDAR) instruments have been used routinely along the central Platte River in Nebraska for more than a decade. Visible wavelength water-penetrating (Kinzel et al. 2007) and conventional near-infrared LiDARS (Woodward 2008) can map topography over spatial extents on the order of square kilometers. Ground-based LiDAR or terrestrial laser scanning is another technology available for mapping emergent sandbars (Collins and Kayden 2006). More recently, Alexander and Zelt (2011) developed a methodology for

measuring sandbar heights with rapid ground surveys using laser levels along the lower Platte River.

Our intent in this article is to describe a set of experimental UAS flights conducted in two study sites along the Platte River in Nebraska. Our goal was to assess the vertical accuracy of emergent sandbar elevations measured by a UAS equipped with a readily available “off the shelf” digital camera, a network of ground control targets, and commercially available photogrammetry software. We also discuss the post-processing workflow of the software, which can significantly impact the overall accuracy of the DEM produced.

Study Sites

We chose two study sites for the evaluation of the T-Hawk survey methodology and accuracy on properties managed by the Platte River Recovery Implementation Program (PRRIP). PRRIP is developing and managing these lands as habitat complexes for threatened and

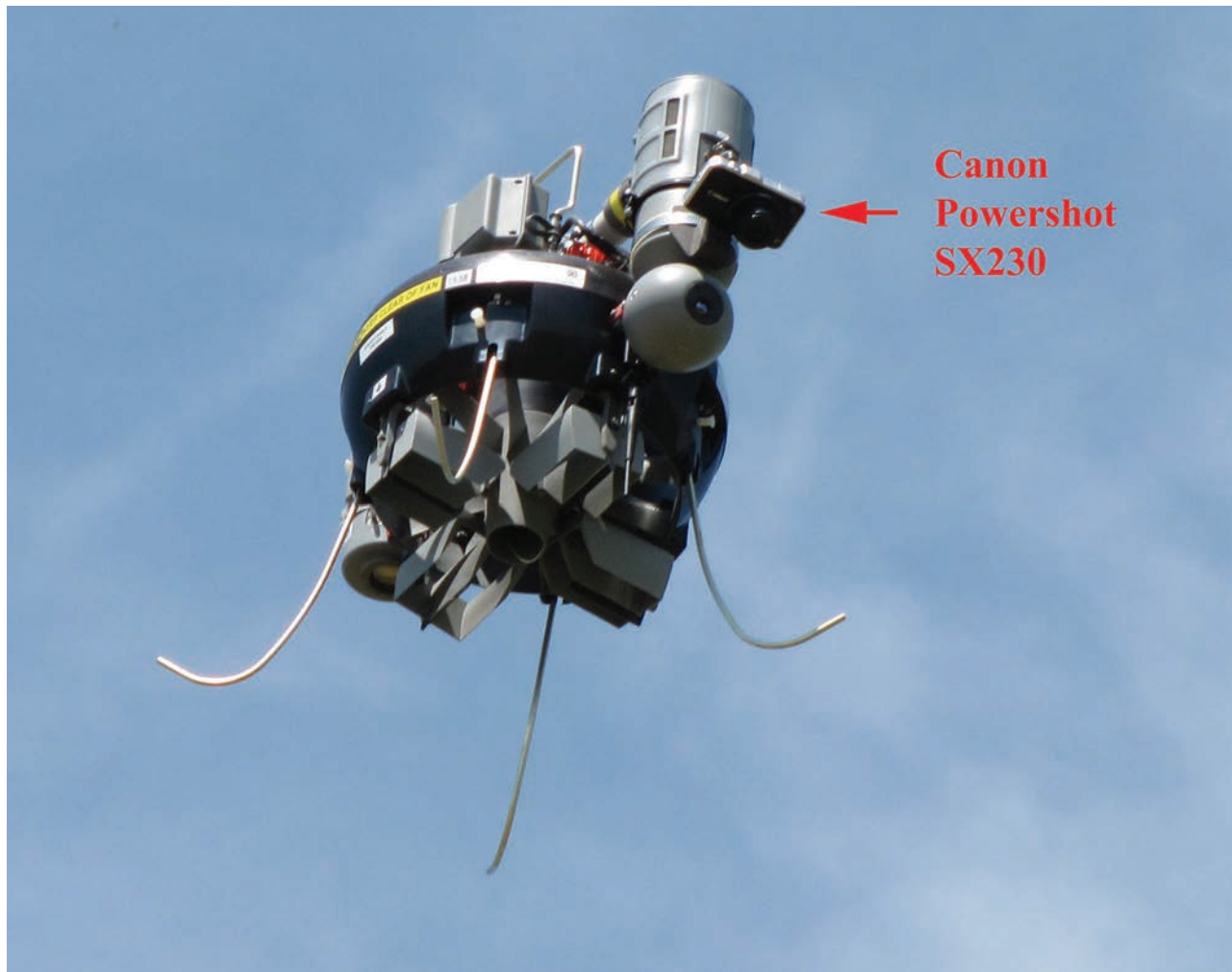


Figure 2. T-Hawk in flight showing the location of the Canon PowerShot sx230HS mounted to the payload pod. Photograph by Mark Bauer, USGS.

endangered species in the Platte River basin. PRRIP has also implemented pilot-scale sediment augmentation projects on these properties to evaluate the logistical aspects of these operations and their cost effectiveness (Platte River Recovery Implementation Program 2011). The downstream site, referred to as the Cottonwood Ranch property, is owned by the Nebraska Public Power District and managed by PRRIP (Fig. 1). PRRIP initiated sand augmentation in the Cottonwood Ranch during the fall of 2012 and used bulldozers to push sand from an adjacent island into the active river channel. The upstream site, referred to as the Dyer property, is both owned and managed by PRRIP (Fig. 1). On the Dyer property, PRRIP installed a sand slurry pump in the fall of 2012 to introduce washed and sorted sand from an adjacent gravel pit into the active river channel.

Methods

UAS System Description

The T-Hawk, also referred to as a gMAV (gasoline Micro Air Vehicle), is operated by the USGS UAS office in Lakewood, Colorado, and was designed and built by Honeywell International to provide aerial reconnaissance and surveillance for the United States Army. The T-Hawk is capable of vertical takeoff and landing and can be controlled manually or autonomously with the use of a preprogrammed flight plan. The standard payload pods include an avionics pod and a payload pod equipped with either a 768×494 pixel electro-optical camera or a 320×240 pixel infrared camera (Fig. 2). The system also contains a GPS antenna for positioning. The T-Hawk can fly up to 72 km per hour, has a range of 10

TABLE 1. Resolution and ground coverage calculated for Canon PowerShot™ SX230HS used in the UAS flights

Altitude above ground level(m)	GSD ^a width (cm)	GSD ^a height (cm)	Photo width (m)	Photo height (m)
61	1.88	1.85	75.22	55.47
91	2.82	2.77	112.84	83.2
121	3.76	3.70	150.45	110.95

^aThe ground sample distance (GSD) is defined as the resolution of the photograph on the ground.

km, a service ceiling of 2,438 m (with 46–122 m typical), and a flight duration of up to 47 minutes (Honeywell International 2009).

Since mapping applications were not a primary design or operational consideration for the T-Hawk, USGS fabricated a camera mount that can be attached to the T-Hawk enabling the use of a lightweight (0.2 kg), inexpensive (~\$300) Canon PowerShot™ SX230HS 12.1 megapixel (3000 × 4000) digital camera pointed at nadir (Fig. 2). Relevant camera parameters include a fixed 5 mm focal length and a wide-angle lens to minimize image distortion. Camera settings included a 0.000625 second shutter speed to minimize blur and the ability to disable the image stabilization feature of the camera. We triggered exposures internally with Canon's CHDK developer's script toolkit and programmed the camera to acquire an image every three seconds. At the nominal flight speed of 24 to 32 km per hour this interval provided sufficient image overlap for the photogrammetry software. We provide the specifications of the imagery including pixel resolution and ground coverage for various altitudes in Table 1.

Image Processing

We processed imagery from the UAS flights at the UAS office in Lakewood, Colorado, with the Agisoft PhotoScan™ software (Agisoft 2013). The software uses multiple overlapping images, sophisticated image matching algorithms, and differences in camera perspective to reconstruct three-dimensional surfaces; this process is often referred to as structure from motion. The first step in the software workflow is the alignment of overlapping images by searching for common points in the

images and matching them together. This initial step allows the software to compute the positions of the camera in each scene. Additionally, a camera calibration and optimization process is implemented that corrects for lens distortions. Ground control points are not required, but if available, can be added to place the scene in a user-defined coordinate system (e.g., Universal Transverse Mercator). A 3D point cloud is generated and then edited to remove erroneous points to reduce projection errors. The next step in the software workflow builds the geometry of the scene, a 3D polygon mesh. The mesh can be edited in a limited fashion in PhotoScan™ at this step or edited extensively, utilizing third-party open-source program software programs such as MeshLab™. The final step involves texturing the mesh and/or the generation of a georeferenced orthophotograph. Depending on the number of images collected and the memory and graphics capabilities of the processing computer, this operation can take from a few hours to a few days to complete. Segments of imagery can also be parsed or “chunked” to increase processing efficiency in the workflow with these chunks reassembled in post-processing to a produce a georectified DEM of the study sites.

UAS Image Acquisition and Ground Control Surveys, Cottonwood Ranch Site

On July 23, 2013, we initiated flights at the river reach adjacent to USGS streamflow-gaging station 06768035, Platte River middle-channel, Cottonwood Ranch, near Elm Creek, Nebraska. (Fig. 1). We selected this site because of the proximity to the gaging station and the 25 river transects that USGS has monitored since 2000 (Kinzel et al. 2006). The authors were joined by staff from the PRRIP executive director's office. A primary concern of PRRIP regarding UAS operations over the river was the potential to interfere with fledging birds. At the Cottonwood Ranch this risk was thought to be low because of the lack of nesting terns and plovers observed in the immediate vicinity. However, based on discussions with PRRIP personnel, this concern was justified at the upstream Dyer site because nesting and fledging birds had been observed at that location. Specifically, lower operating altitudes of approximately 61 m above ground level (AGL) were believed to have the potential to interfere with fledging birds.

We flew the T-Hawk at multiple altitudes in the Cottonwood Ranch, 121, 91, and 61 m AGL, to collect imag-

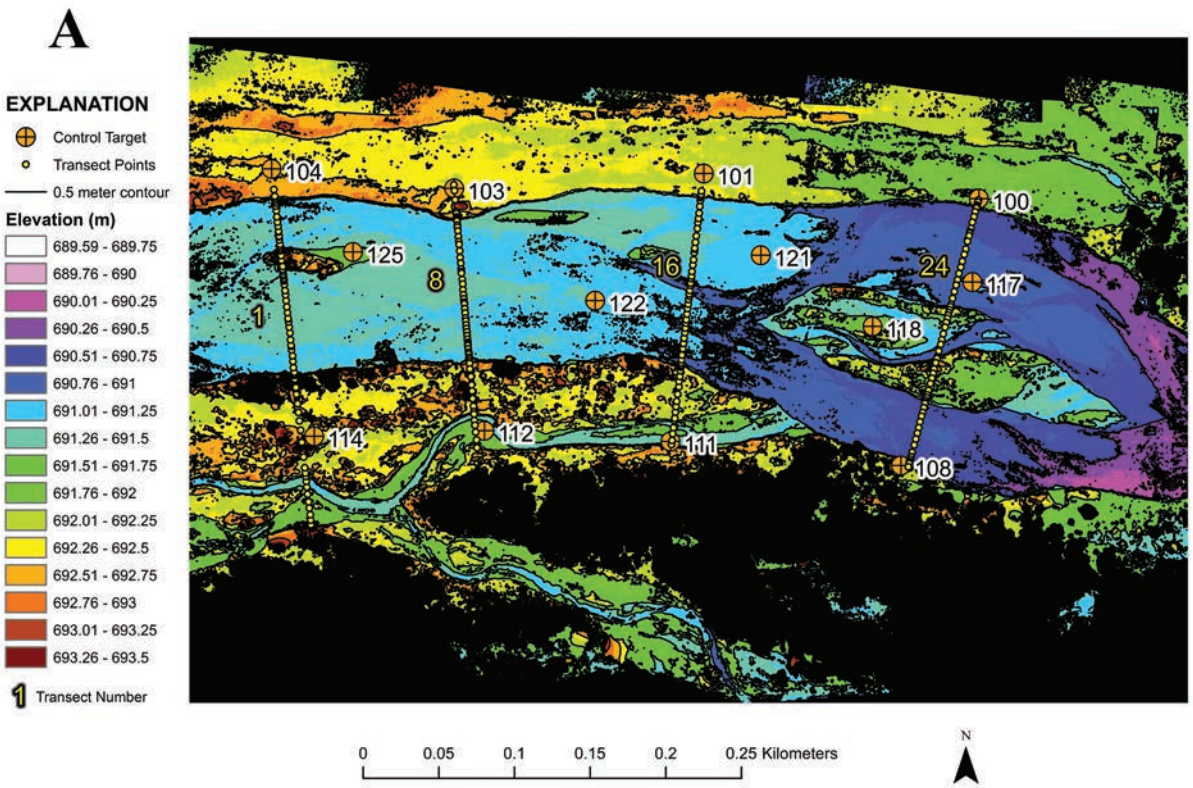


Figure 3A. Digital elevation model of the Cottonwood Ranch study reach, showing the location of ground control points used in processing and transect points used for elevation comparison.

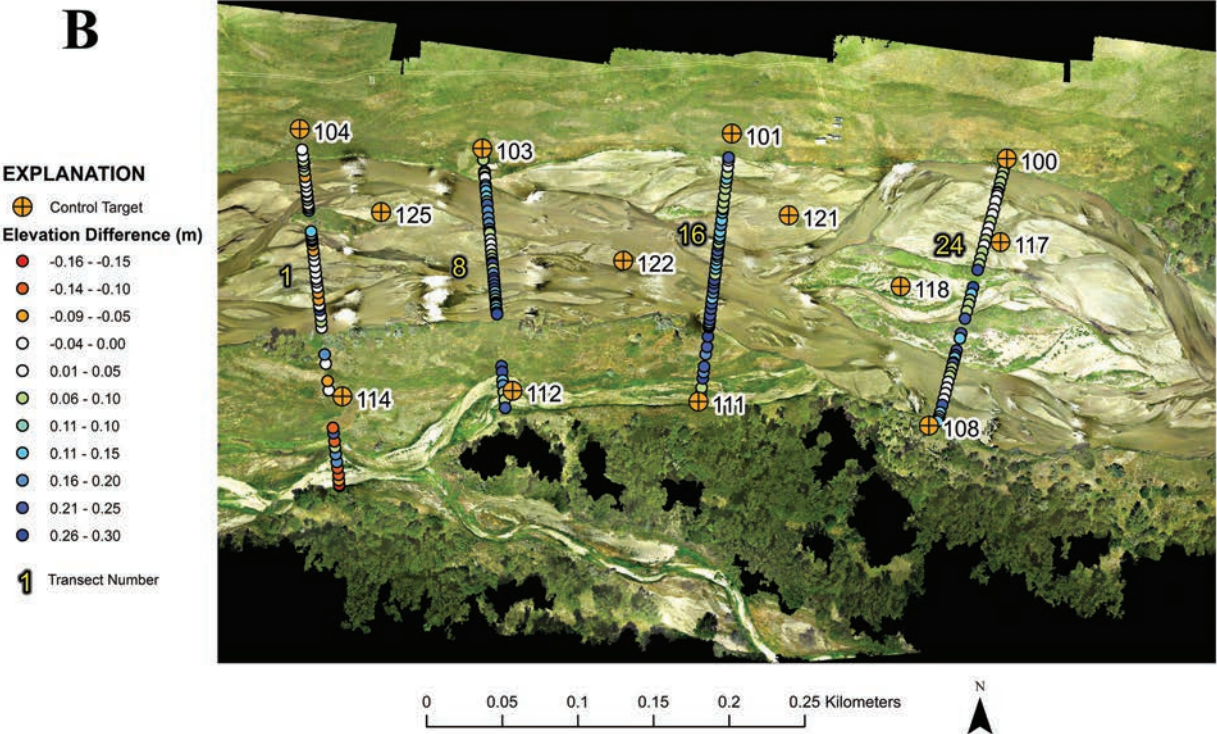


Figure 3B. Digital orthophotograph of the Cottonwood Ranch study reach, showing the location of ground control targets used in processing and transect points used for elevation comparison. The elevation difference is the RTK-GPS elevation subtracted from the DEM elevation at each transect point.

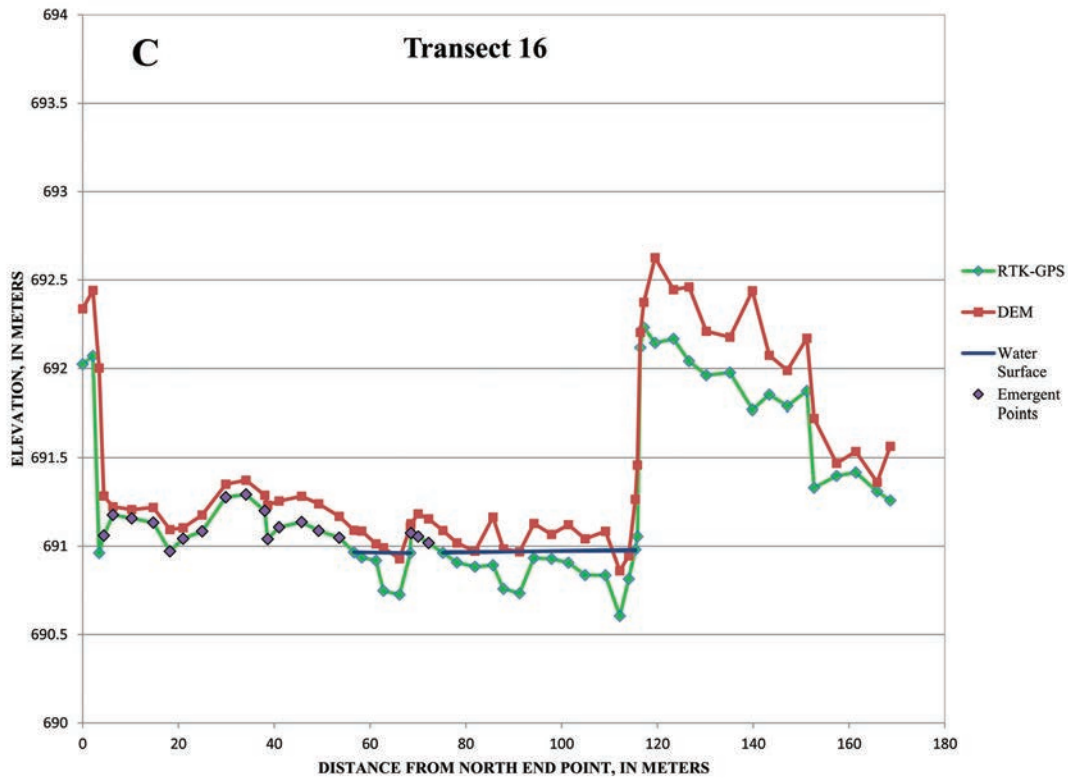


Figure 3C. 2D plot of transect 16, Cottonwood Ranch study reach.

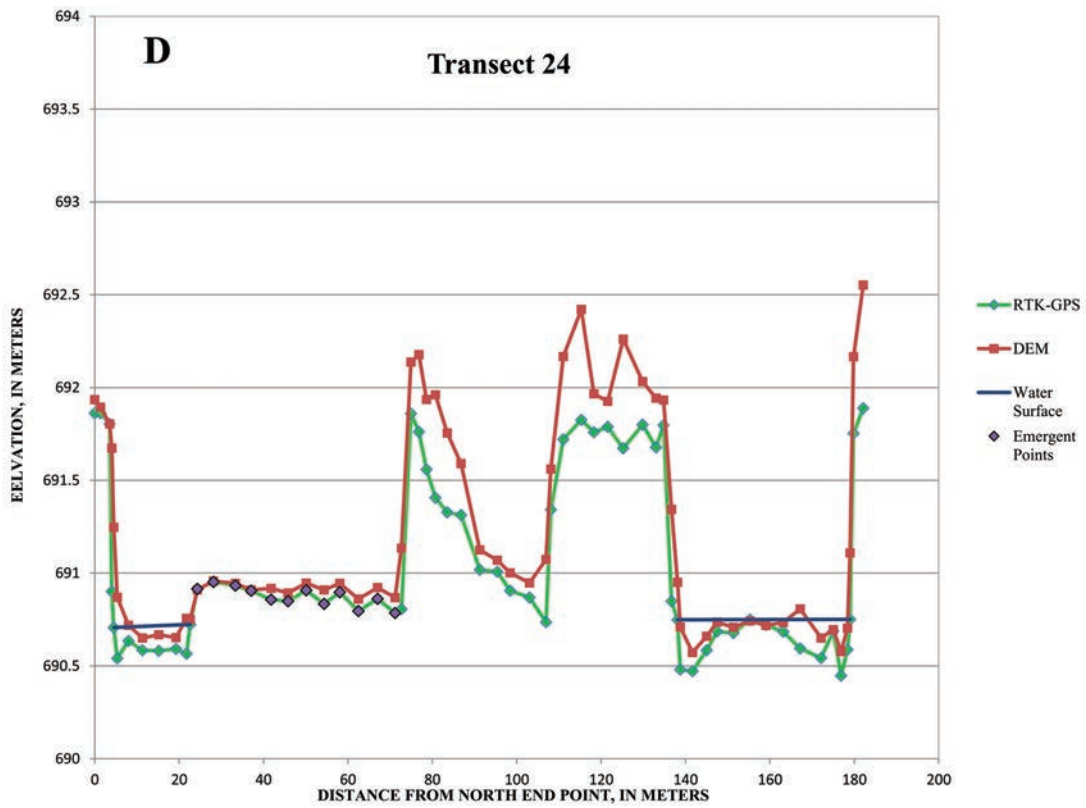


Figure 3D. 2D plot of transect 24, Cottonwood Ranch study reach.

ery for photogrammetric processing. However, only the imagery collected from the 61 and 91 m elevations was used to generate the DEM (in meters above the North American Vertical Datum of 1988) and the ground truth comparison presented here. The flight lines created in the mission planning software extended in an east–west direction parallel with the river and also in a north–south direction, providing 60% along-track and 50% cross-track overlap for image processing. Provisional streamflow during the data collection was approximately 3.4 m³/s at the Cottonwood Ranch streamflow gage (USGS National Water Information System, <http://water.data.usgs.gov/nwis>). The mean depth observed along the surveyed transects was 0.12 m ($n = 87$). These low flows provided large areas of emergent sandbars in the study reach.

We registered the aerial imagery by placing four ground control targets along the north bank of the river and four along the south bank of the river. (While the T-Hawk has an onboard GPS, its accuracy was thought to be insufficient for this application.) Each target consisted of an orange 19 L bucket lid with a 1.27 cm diameter hole drilled through the center. The target was anchored using a 0.61 m length of 1.27 cm diameter rebar pounded through the hole. To increase visibility of the targets in the imagery, a compact disc painted a flat black color was slipped over the top of the rebar and rested on the surface of the lid. Five additional targets were placed on emergent bars spaced through the mapping area. We surveyed the horizontal and vertical positions of each target with a real-time kinematic global positioning system (RTK-GPS). The precisions of the RTK-GPS system reported by the manufacturer are approximately 8 mm in the horizontal and 15 mm in the vertical (Trimble Navigation 2013). We also collected topographic surveys, oriented perpendicular to the river along four monitoring transects (1, 8, 16, and 24) using the RTK-GPS instrument (Figs. 3A–3D).

Dyer Site

On July 24, 2013, we flew multiple missions with the T-Hawk along the Dyer property. A representative from the PRRIP was present on this day to observe bird response. Our observations indicated that the lowest altitude flights (~61 m AGL) did not appear to disturb birds near the river. Provisional streamflows measured at the USGS streamflow-gaging station 06768000 Platte River near Overton, Nebraska (Fig. 1), were approximately 2.8

m³/s (USGS National Water Information System, <http://water.data.usgs.gov/nwis>). The average depth measured in submerged areas was also 0.12 m ($n = 56$). We flew the T-Hawk in a pattern similar to the Cottonwood Ranch flight plan, at 121, 91, and 61 m AGL. As with the Cottonwood site, we only used the imagery collected at 61 and 91 m elevations to generate the orthophotograph and the DEM used in the analysis. We established and surveyed with RTK-GPS a total of 15 ground control targets: five on the north bank, five on the south bank, and five additional targets on emergent bars. Additionally, we collected river transect surveys with RTK-GPS along three of the sediment augmentation monitoring transects (3, 4, and 5) established in the site (Platte River Recovery Implementation Program 2011) (Figs. 4A–4E).

Results

Cottonwood Ranch Site

The targets that we retained in the creation of the DEM and their root mean square errors in three dimensions are provided in Table 2A. We paired RTK-GPS transect points with coincident locations in the DEM generated from the photogrammetry software in a geographic information system (Fig. 3A). The differences between the two elevations (DEM–RTK-GPS) at each RTK-GPS point were overlain on the orthophotograph and are shown in Figure 3B. The survey points with differences between –0.05 and 0.05 m are colored white to easily identify where areas of good correspondence were located. Warmer colors indicate where the elevation of the DEM fell below the elevation of the RTK-GPS point. These differences were not common and were predominantly observed in vegetated areas at the south end of transect 1. Cooler colors represent areas where the DEM elevation fell above the RTK-GPS elevation. Emergent sandbar points used in the vertical accuracy assessment were defined to include points along the ground survey that fell between wetted areas but were not covered in vegetation. These points are colored purple in the 2D elevation plots (Figs. 3C and 3D). Transect 16 showed the greatest error between RTK-GPS emergent sandbar point elevations and the DEM (Fig. 3C). The errors in the DEM along this transect suggest a consistent vertical bias, but the general shape of the bar surface appears to be represented. The error in this transect relative to the other transects could be attributed to eliminating two ground control points located near this transect, 121 and 122, from the processing procedure. As was mentioned pre-

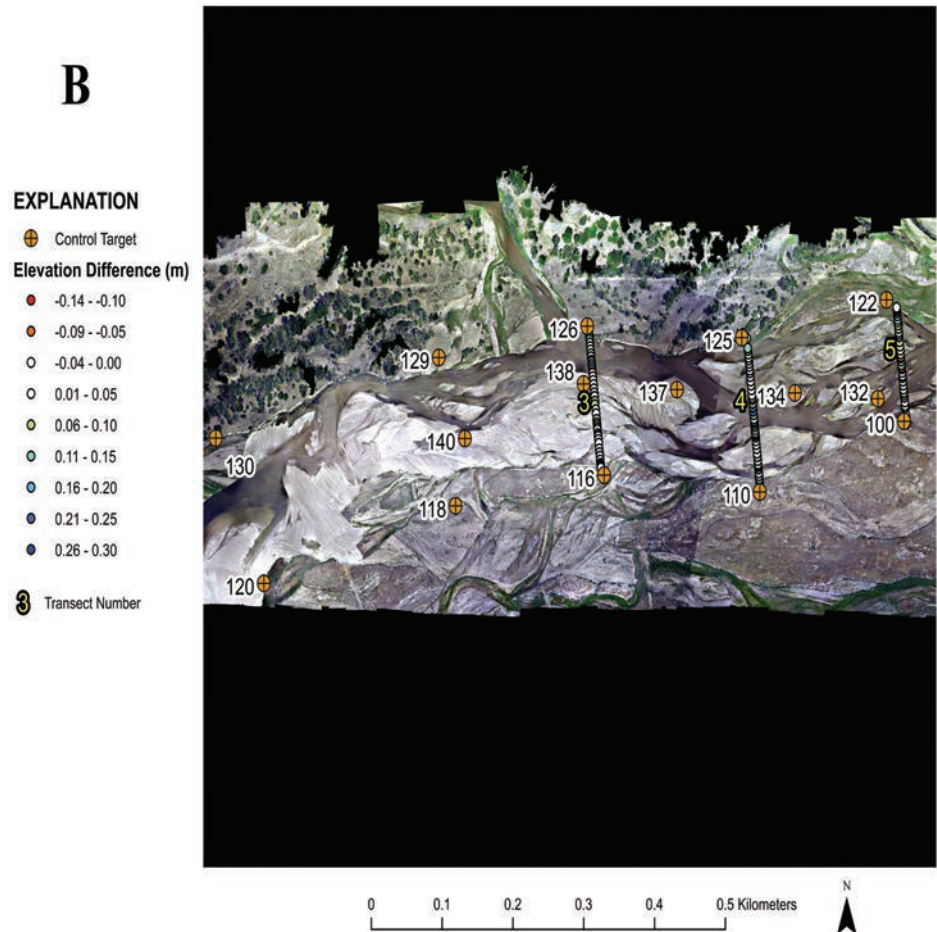
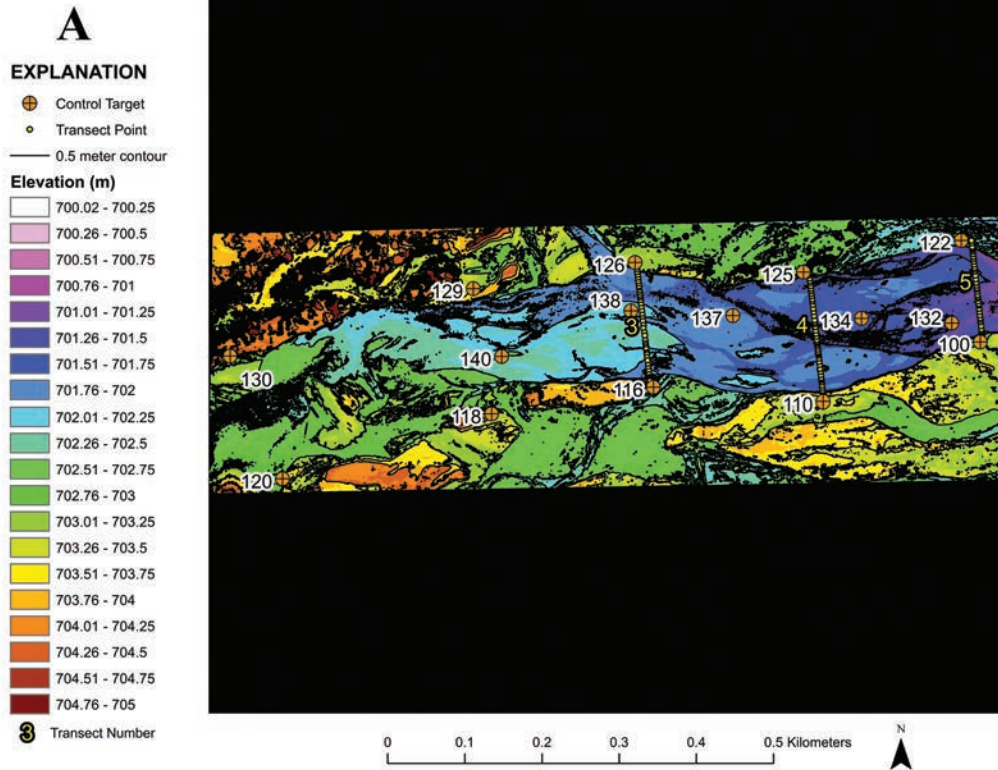


Figure 4A (above). Digital elevation model of the Dyer reach, showing the location of ground control points used in processing and transect points used for elevation comparison.

Figure 4B (right). Digital orthophotograph of the Dyer reach, showing the location of ground control targets used in processing and transect points used for elevation comparison. The elevation difference is the RTK-GPS elevation subtracted from the DEM elevation at each transect point.

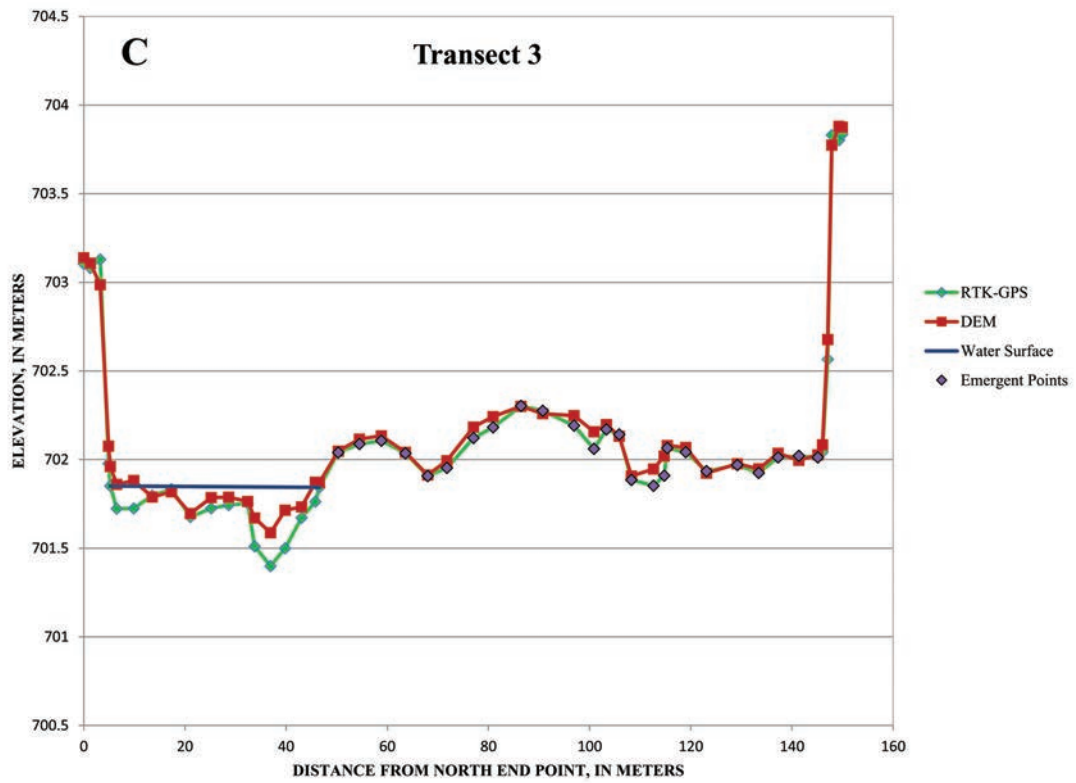


Figure 4C. 2D plot of river transect 3, Dyer reach.

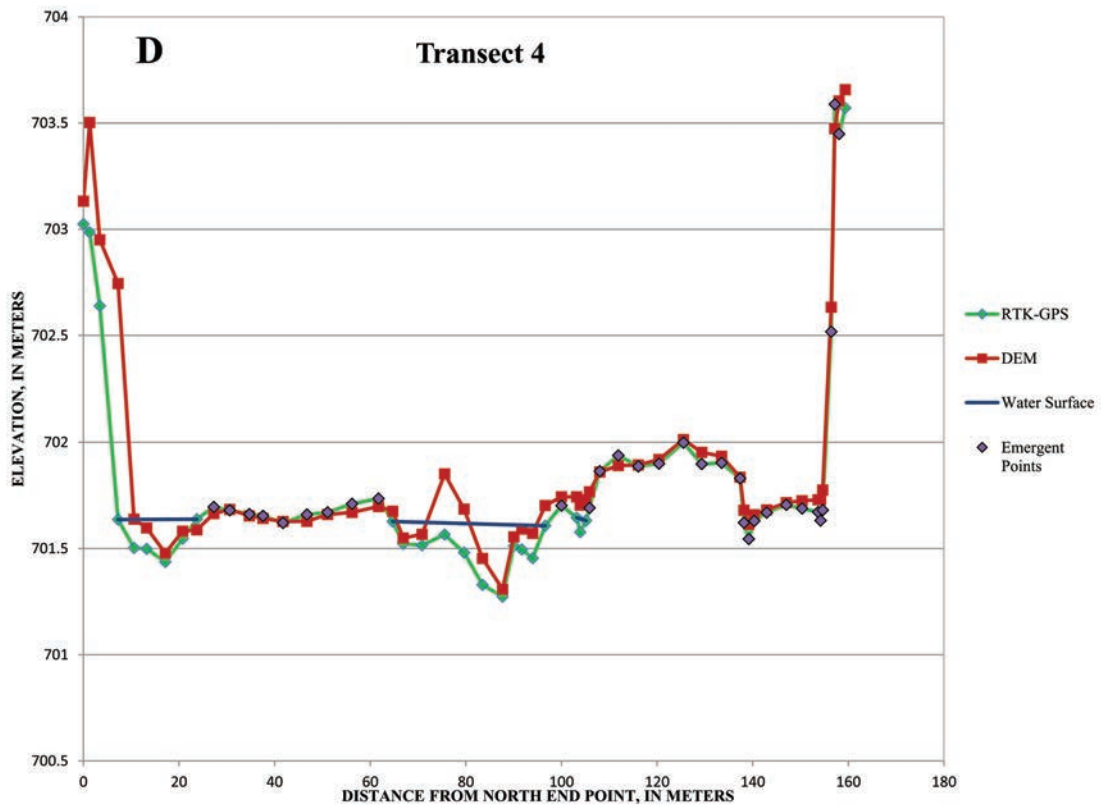


Figure 4D. 2D plot of river transect 4, Dyer reach.

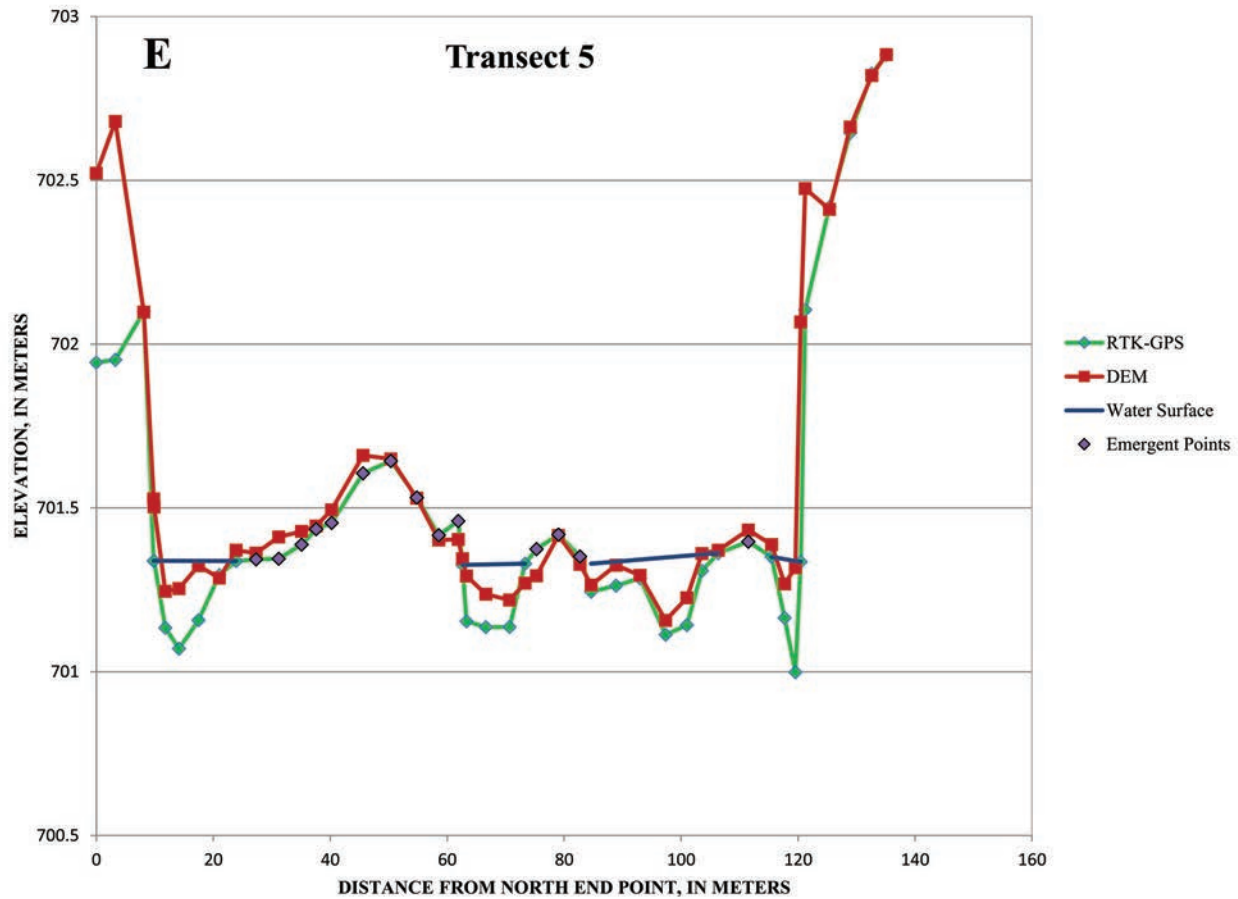


Figure 4E. 2D plot of river transect 5, Dyer reach.

viously, this can reduce the overall error of the project but appears to have introduced local errors in the DEM along this transect. While vegetated bars were not common in this reach, the center portion of transect 24 (between the 70 and 140 m stations in Fig. 3D) was covered in vegetation. There were some points extracted from the DEM that fell beneath the surveyed water-surface elevation, which may indicate that the photogrammetry software was able to generate a surface in some of the submerged areas in the channel. We report the root mean square error in elevation for the emergent points along the surveyed transects in Table 2B.

Results

Dyer Site

We report the targets retained in the creation of the DEM and their errors in Table 3A. We used the same analysis procedure to evaluate the Dyer DEM (Fig. 4A). As with

the Cottonwood Ranch survey, we found only a few elevation differences that indicated the DEM elevation was below the RTK-GPS elevation. These differences were most pronounced in the wet portion of the channel or along the banks. Elevation differences where the DEM elevation was above the RTK-GPS elevation occurred more frequently and were present in the wet portions of the channel (Figs. 4B, 4C, 4D, and 4E). Additional examples of the DEM elevation extending below the water surface are in Figs. 4C–E. We report the root mean square error in elevation for the emergent points along the surveyed transects in Table 3B.

The sediment augmentation operations at the Dyer property left large stockpiles of sand. We flew the T-Hawk at 61 and 91 m over these stockpiles to gather imagery, create a DEM and estimate their volume (Fig. 5). To aid in registration of the UAS imagery and DEM generation, we placed three ground control targets to the north, west, and south sides of the piles. The errors

TABLE 2A. Root mean square errors (RMSE) for the targets used in the Cottonwood Ranch PhotoScan™ project workflow

Target	X-RMSE (m)	Y-RMSE (m)	Z-RMSE (m)
100	-0.005	0.030	-0.029
101	-0.001	-0.032	0.010
103	0.030	-0.003	0.017
104	-0.024	0.037	-0.034
108	0.029	0.026	-0.029
111	-0.017	-0.025	0.020
112	-0.019	-0.004	0.029
114	0.011	-0.020	-0.039
118	-0.031	-0.020	0.027
125	0.020	0.020	0.039
Total	0.021	0.024	0.029

TABLE 2B. Root mean square error (RMSE) in elevation for the emergent points along each surveyed transect

Transect	1	8	16	24
Z-RMSE (m)	0.05	0.06	0.12	0.05
<i>n</i>	13	6	18	12

TABLE 3A. Root mean square errors (RMSE) for the targets used in the Dyer PhotoScan™ project workflow

Target	X-RMSE (m)	Y-RMSE (m)	Z-RMSE (m)
100	0.050	0.043	-0.019
110	-0.018	-0.025	0.009
116	-0.020	0.015	0.028
118	-0.013	-0.027	-0.014
122	-0.048	-0.041	0.012
125	0.020	-0.007	-0.013
126	0.002	0.020	-0.022
129	-0.005	-0.003	0.017
130	0.021	0.019	-0.002
132	0.026	0.025	-0.013
134	-0.006	-0.023	0.011
137	-0.008	0.014	0.011
138	-0.009	0.006	0.021
140	0.013	-0.016	-0.027
Total	0.023	0.023	0.017

TABLE 3B. Root mean square error (RMSE) in elevation for the emergent points along each surveyed transect

Transect	3	4	5
Z-RMSE (m)	0.05	0.06	0.04
<i>n</i>	25	33	14

TABLE 4. Root mean square errors (RMSE) for the targets used in the Dyer stockpile PhotoScan™ project workflow

Target	X-RMSE (m)	Y-RMSE (m)	Z-RMSE (m)
142	-0.00008	-0.03	0.00006
144	-0.04	0.01	0.04
146	0.04	0.03	-0.0002
Total	0.03	0.02	0.0001

for each target are provided in Table 4. Assuming a base elevation of 705 m, we calculated the total volume of the piles to be approximately 6,070 m³.

Discussion

The accuracy of the survey methodology presented herein is inextricably linked to both the quality of the images collected by the UAS platform and the post-processing workflow. Projects created in the PhotoScan™ software use a texture matching algorithm to find common tie points between images for alignment. During the automated process of tie point generation, the program will identify tie points that, because of motion or vibration of the camera, are from blurred imagery. The reduced resolution in these blurred images causes mismatches in pixel location between images, which in turn introduces error in the alignment process. The error, expressed in pixels, can be thought of as a quantitative measure of the ability of that alignment to correct for the lens distortion of the camera. The challenge is to gradually remove tie points to minimize errors in the alignment but retain enough tie points to generate a surface model with sufficient density for a particular application. By iterating on the selection of tie points used in the alignment, an error minimum can be found that produces an optimal alignment.

A second component that influences the overall accuracy of the project workflow is the registration of

EXPLANATION

- ⊕ Control Target
- 1 meter contour

Elevation (m)

700.03 - 700.5
700.51 - 701
701.01 - 701.5
701.51 - 702
702.01 - 702.5
702.51 - 703
703.01 - 703.5
703.51 - 704
704.01 - 704.5
704.51 - 705
705.01 - 705.5
705.51 - 706
706.01 - 706.5
706.51 - 707
707.01 - 707.5
707.51 - 708
708.01 - 708.5
708.51 - 709
709.01 - 709.5
709.51 - 710
710.01 - 710.5
710.51 - 711
711.01 - 711.5
711.51 - 712

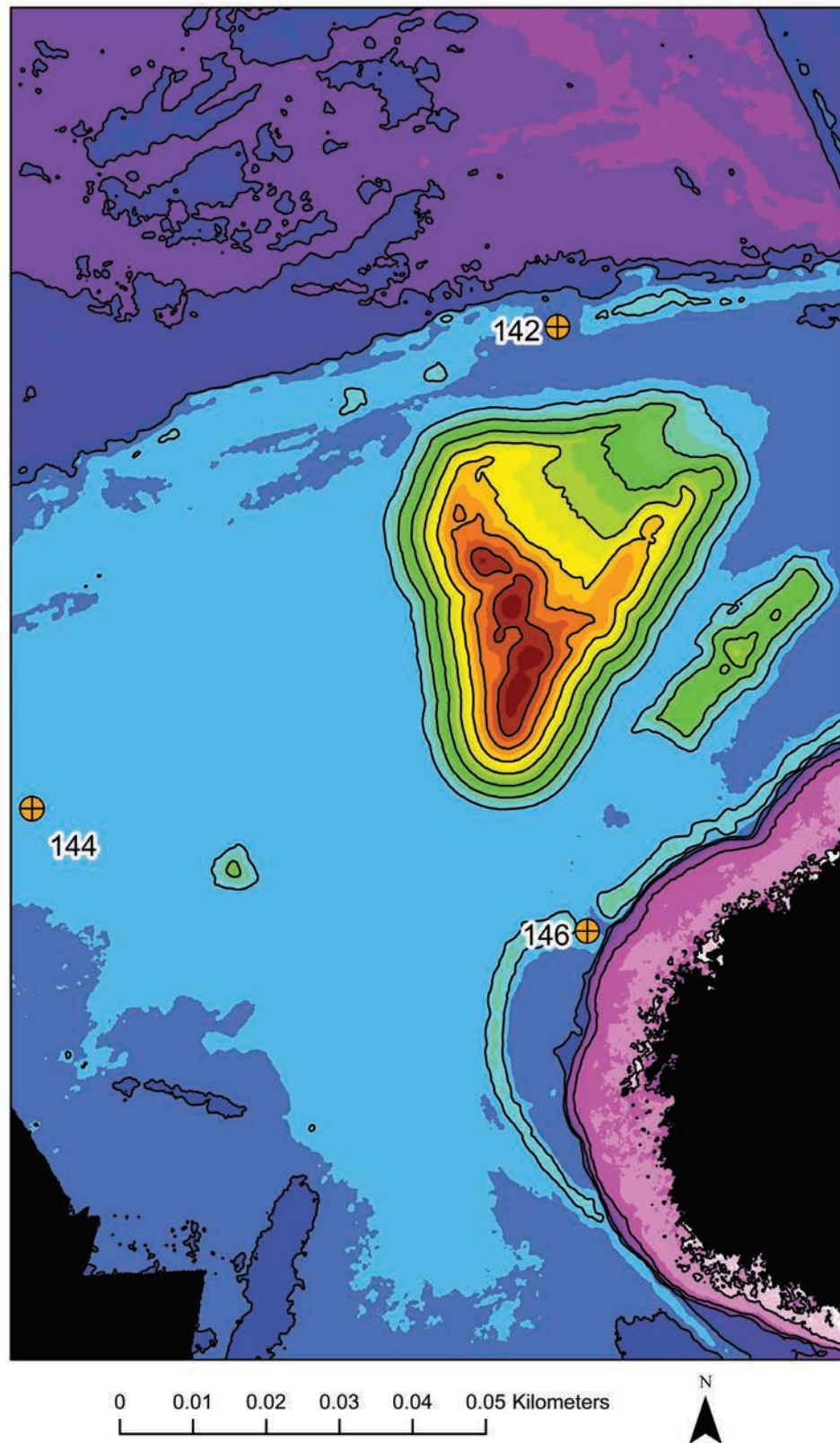


Figure. 5. Digital elevation model of sand piles on the Dyer property used for the pilot-scale sediment augmentation project.

ground targets to transform the aligned imagery from an arbitrary coordinate system to real-world coordinates. We found that after registration some targets had large errors relative to others. The errors in these targets could have been introduced by blurred images that made the registration more difficult and therefore less accurate. Additionally, any errors in the ground survey coordinates can also introduce errors in target registration. Eliminating targets with a high relative error reduced the overall error in the set of targets ultimately used in the transformation (Tables 2A, 3A, and 4).

Overall, we found that wet portions of the river channel produced higher relative elevation errors than those on emergent bars. This is not particularly surprising as it is recommended that users of PhotoScan™ should avoid transparent objects. Shiny objects that can occur with sun glint off the water surface are also discouraged. Elevations across vegetated islands and along bank areas also produced high relative errors. The PhotoScan™ software was not capable of determining ground elevations under dense bar, bank, or island vegetation. Our ground surveys did not attempt to measure the vegetation height in these areas. This would be an interesting application of a UAS survey but is beyond the scope of this paper.

Conclusions

We conducted experimental flights over reaches of the Platte River, Nebraska, using a UAS system developed for the military and modified for an inexpensive digital camera payload. While conventional LIDAR surveys can provide elevation data over multiple kilometers of river channel efficiently and with high accuracy, on the order of centimeters, these flights are relatively expensive (a LIDAR acquisition over an approximate 145 km reach of the Platte River, which includes the simultaneous collection of color-infrared imagery, can approach \$100,000, according to the Platte River Recovery Implementation Program). Thus, in the case of the PRRIP, these surveys are collected only on an annual basis.

In contrast, the operational cost of UAS survey is currently estimated to be on the order of several thousand dollars, including the travel cost for a minimum crew of three over several days in the field and the costs associated for a single individual to process the data. Due to the endurance of the UAS used in this study and requirements for continuous visual contact, a UAS survey is most efficiently conducted over short (1–2 km) river

reaches. We demonstrate with the UAS described in this paper that the vertical accuracy is highly dependent on the quality of imagery and the post-processing workflow. If enough accurate ground control is established in the site, errors can be minimized in the topographic model and can approach the centimeter-level vertical precisions of aerial LIDAR. Future advances in UAS hardware (GPS and inertial navigation systems) may enable increased precision in the positioning of imagery, reducing or perhaps at some point even eliminating the need for ground control targets. Those advances, combined with more sophisticated payloads that include higher resolution imagers and/or active ranging sensors, promise to make this rapidly evolving technology a viable option for relatively low-cost environmental monitoring.

.....
Paul Kinzel, US Geological Survey, Geomorphology and Sediment Transport Laboratory, Golden CO 80403, pjkinzel@usgs.gov

Mark Bauer, Parallel Inc., Lakewood CO 80228

Mark Feller, US Geological Survey, Unmanned Aircraft Systems Office, Lakewood CO 80225

Christopher Holmquist-Johnson, US Geological Survey, Fort Collins Science Center, Fort Collins CO 80526

Todd Preston, Parallel Inc., Lakewood CO 80228

Acknowledgments

We thank the Platte River Recovery Implementation Program for allowing access to the habitat complexes they own and manage. James Jenniges from the Nebraska Public Power District assisted in granting us permission and access to the Cottonwood Ranch property. Tommy Noble (Bureau of Land Management) provided support with photogrammetric processing and analysis. Susan Goplen (USGS National UAS Project Office) assisted in obtaining the certificate of authorization from the Federal Aviation Administration. We also thank Jeff Sloan (USGS National UAS Project Office) for his support of this project. Any use of trade, firm, or product name is for descriptive purposes only and does not imply endorsement by the United States government.

References

- Agisoft. 2013. *Agisoft PhotoScan User Manual Professional Edition*, version 0.9.1.
- Alexander, J. S., and R. B. Zelt. 2011. "Sandbar Dynamics in the

- Lower Platte River Pilot Study-Methods and Initial Results." Paper presented at 2011 Climate, Water and Ecosystems Conference, Lincoln NE.
- Ball, M. 2013. "What Are the Top Ten Civilian Uses of Drones that Don't Impinge Privacy?" <http://www.sensorsandsystems.com/dialog/perspectives/30861-what-are-the-top-ten-civilian-uses-of-drones-that-don%e2%80%99t-impinge-privacy.html>.
- Collins, B. D., and R. Kayden. 2006. "Applicability of Terrestrial LIDAR Scanning for Scientific Studies in Grand Canyon National Park, Arizona." US Geological Survey, Open-File Report 2006-1198. Reston VA.
- Elliott, C. M. 2011. "Geomorphic Classification and Evaluation of Channel Width and Emergent Sandbar Habitat Relations on the Lower Platte River, Nebraska." USGS Scientific Investigations Report 2011-5028. Reston VA.
- Elliott, C. M., B. L. Huhmann, and R. B. Jacobson. 2009. "Geomorphic Classification of the Lower Platte River, Nebraska." USGS Scientific Investigations Report 2009-5198. Reston VA.
- Honeywell International. 2009. "Gasoline Micro Air Vehicle (gMAV) Capabilities Brief."
- Kinzel, P. J., J. M. Nelson, and A. K. Heckman. 2006. "Channel Morphology and Bed-Sediment Characteristics Before and After Riparian Vegetation Clearing in the Cottonwood Ranch, Platte River, Nebraska, Water Years 2001-2004." USGS Scientific Investigations Report 2005-5285. Reston VA.
- Kinzel, P. J., J. M. Nelson, and A. K. Heckman. 2009. "Response of Sandhill Crane (*Grus canadensis*) Riverine Roosting Habitat to Changes in Stage and Sandbar Morphology." *River Research and Applications* 25:135-52.
- Kinzel, P. J., C. W. Wright, J. M. Nelson, and A. R. Burman. 2007. "Evaluation of an Experimental LIDAR for Surveying a Shallow, Braided, Sand-Bedded River." *Journal of Hydraulic Engineering* 133:838-42.
- Legleiter, C. J., P. J. Kinzel, and B. T. Overstreet. 2011. "Evaluating the Potential for Remote Bathymetric Mapping of a Turbid, Sand-Bed River: 2. Application to Hyperspectral Image Data from the Platte River." *Water Resources Research* 47:w09532.
- Lejot, J., C. Delacourt, H. Piégay, T. Fournier, M. L. Trémélo, and P. Allemand. 2007. "Very High Spatial Resolution Imagery for Channel Bathymetry and Topography from an Unmanned Aerial Platform." *Earth Surface Processes and Landforms* 32:1705-25.
- Platte River Recovery Implementation Program. 2011. *Sediment Augmentation Pilot-Scale Management Action Monitoring and Analysis Data Plan*. Kearney NE.
- Strong, L. 2007. "Assessment of Least Tern and Piping Plover Habitats on the Missouri River Using Remote Sensing." USGS Fact Sheet 2007-3087. Reston VA.
- Trimble Navigation. 2013. "Trimble R8 GNSS System Datasheet." http://trl.trimble.com/docushare/dsweb/Get/Document-140079/022543-079m_Trimbler8gNSS_ds_0413_lr.pdf.
- Woodward, B. K. 2008. "Streamflow and Topographic Characteristics of the Platte River near Grand Island, Nebraska, 1938-2007." USGS Scientific Investigations Report 2008-5106. Reston VA.